DISTRIBUTION OF OXYGEN IN SILICON AND ITS EFFECTS ON ELECTRONIC CHARACTERISTICS ON A MICROSCALE

H. C. Gatos, P. Rava, and J. Lagowski
Massachusetts Institute of Technology
Cambridge, Massachusetts

ABSTRACT

The microdistribution of oxygen in silicon was obtained by scanning IR absorption in as-grown Czochralski crystals. The crystals were subsequently submitted to various heat treatments. The profiles of the generated thermal donors were determined by spreading resistance measurements. Contrary to the prevailing views, it was found that the concentration of the activated thermal donors is not strictly a function of the oxygen concentration, but depends strongly on an additional factor, which was shown to be associated with vacancy concentration. These conclusions could only be reached on the basis of microscale characterization. In fact, commonly employed macroscale analysis has led to erroneous conclusions.

INTRODUCTION

Oxygen is invariably present in Czochralski-grown Si crystals at concentration levels in the vicinity of $10^{18}/cm^3$. It originates from the interaction of molten Si with the SiO_2 crucible and, like all impurities in Si, oxygen is not uniformly distributed (ref. 1). It is a highly undesirable impurity in a number of device applications.

The interstitial oxygen, in as-grown crystals is electrically inert. It has been generally accepted for many years that the concentration of oxygen donors activated upon heat treatment at 450°C is directly related to the interstitial oxygen concentration. Although quantitative relationships have been proposed based on macroscale (average) determinations of oxygen concentration by IR absorption and the (mean) activated oxygen donor concentration (ref. 2) they have not been generally confirmed (ref. 3).

In the present study, by correlating the oxygen concentration and activated oxygen donors in Si on a microscale, the main uncertainties stemming from earlier macroscale measurements are, for the first time, clarified.

EXPERIMENTAL

Oxygen concentration microprofiles were obtained by scanning IR absorption employed earlier for the determination of carrier concentration microprofiles (refs. 4,5). As seen in Fig. 1, it consists of a tunable CO_2 laser, an optical system for monitoring the power and wavelength of the laser beam, a stage with x-y motion and an IR detector. The wafer was mounted on the stage and the intensity of the collimated beam (~30 μm in diameter) passing through the wafer was measured as a function of the position along the sample.

The laser beam was chopped in order to use lock-in detection of the signal. Since the smallest wavelength attainable with the CO_2 laser was 9.17 μ, whereas the peak of the oxygen absorption band is at 9.04 μm, a ratio of α_o(9.04 μm)/α(9.17 μm) = 1.95 was obtained using a Fourier transform spectrometer; this ratio was used for making the necessary correction in determining the oxygen concentration (ref. 6).

Both parallel faces of the Si samples were polished to a mirror finish and coated with a quarter wavelength zinc sulfide antireflection coating to reduce the reflection coefficient and avoid interference caused by multi-reflections of the light beam inside the sample. This coating was employed by Ohsawa et al (ref. 3) who have also recently obtained oxygen profiles in Si crystals by scanning IR absorption using a semiconductor laser.

Carrier concentration profiles were determined from spreading resistance measurements at 10 μm intervals.

An oxygen concentration microprofile taken parallel to the growth direction 6 mm from the periphery of the crystal is shown in Fig. 2a. It is seen that the oxygen concentration fluctuates from about 1 x 10^{18} to 1.5 x $10^{18}/cm^3$. The fluctuations are more random than periodic, indicative of turbulence convection in the melt during growth (ref. 1). The crystal was (commercial) dislocation-free, Czochralski-grown p-type, B-doped with a mean carrier concentration of 1.5 x $10^{15}/cm^3$. A carrier concentration profile along the IR transmission scan of Fig. 1a exhibited essentially no fluctuations, typical for B-doped crystals (ref. 1).

Subsequently, the Si slice was heat treated at 450°C for 4 hours, to activate oxygen donors, and a spreading resistance scan was taken along the line of the IR absorption scan. The results are shown in Fig. 2b. The hole concentration is decreased from its original value of 1.5 x 10^{15} by the amount of activated oxygen donors. It is seen that the oxygen and carrier concentration profiles exhibit in general similar features. As an average the donor concentration is about three orders of magnitude smaller than the oxygen concentration.

A close examination of profiles 2a and 2b shows that in some locations there is no direct correspondence between oxygen and activated donor concentrations. For example, in location B the concentration of oxygen is greater than that in location A, whereas the corresponding oxygen donor concentration in B is smaller than in A. Similarly, in location C the oxygen concentration exhibits a peak which does not appear in the carrier concentration profile.

Upon heat treatment of the slice at 650°C for 4 hours the oxygen donors, as expected, were annihilated; the slice was then heat treated again at 450°C for 8 hours. The resulting carrier concentration profile is shown in Fig. 3c. It is seen that in this case the overall activated donor concentration is significantly smaller than before the 650°C heat treatment. Here again (as in Fig. 2b) in locations A and B there is no direct correspondence between oxygen and oxygen donor concentration. Furthermore, the oxygen concentration peak in location C becomes visible in Fig. 2c, whereas it was not present in Fig. 2b.

It is important to point out that with each subsequent heat treatment of the same slice at 650°C and then at 450°C the concentration of the activated oxygen donors continuously decreased. In the present case after a cumulative heat treatment of about 15 hours at 650°C the oxygen donor concentration activated by heat treatment at 450°C for a few hours was greatly reduced.

The discrepancies between oxygen and oxygen donor concentrations were found to be very pronounced near the periphery of the crystal. An oxygen concentration profile taken parallel to the growth direction 4.5 mm from the periphery of the same crystal and the corresponding carrier concentration profile taken after heat treatment at 450°C for 4 hours are shown in Figs. 3a and 3b, respectively. As is well known, the mean concentration of the oxygen is smaller near the periphery than towards the center of the crystal.

The striking result presented in Fig. 3b is that in entire regions no oxygen donors were formed, and in fact the carrier concentration in some of these regions ($\sim 1.5 \times 10^{15}/cm^3$) is the same as prior to the heat treatment. There are, of course, regions in which activation of oxygen donors took place. After the oxygen donors were annihilated by a heat treatment of 650°C for 4 hours, the slice was heat treated again at 450°C for 8 hours. The resulting carrier concentration profile is shown in Fig. 3c. It is seen that activation of oxygen donors took place in regions in which activation was not pronounced or not observed after the first heat treatment (region B, for example). In regions where pronounced activation took place after the first heat treatment the concentration of oxygen donors decreased following the second 450°C heat treatment (for example, region A) consistent with results presented in Fig. 1.

With subsequent heat treatments of the same slice at 650°C and then at 450°C the concentration of the oxygen donors in the regions where activation had not taken place after the first heat treatment continued to increase to a maximum value and then decreased eventually reaching very small values Fig. 3d). Thus, the oxygen activation behavior near the periphery and towards the center of the crystal is shown in Fig. 4.

A series of oxygen profiles taken on the same silicon crystal at various distances from the periphery (abscissa) are shown in Fig. 5. It is seen that the variations in oxygen concentration are more pronounced near the periphery of the crystal than near the center. It is further seen that certain patterns of inhomogeneities persist from the periphery to the center of the crystal. The corresponding carrier concentration profiles are shown in Fig. 6. Here again it is apparent that near the periphery there are extended regions in which no donor activation took place during the initial heat treatment at 450°C.

DISCUSSION

It is apparent that the concentration of oxygen is not necessarily the controlling factor in the thermal activation of oxygen donors. Although their quantitative analysis is being pursued, the present results, at least qualitatively, are in good agreement with a proposed model (ref. 7) which postulates the interaction of interstitial oxygen with Si vacancies.

According to this model, during thermal activation of donors the interstitial oxygen, O_i, first occupies a Si vacancy, V_{Si}, and then it combines with a neighboring Si vacancy V_n.

$$O_i + V_{Si} \rightarrow O_{Si} \qquad (1)$$

$$O_{Si} + V_n \rightarrow O_{Si}^{+}V_n^{-} \qquad (2)$$

The oxygen-vacancy complex is then readily ionized as a donor:

$$O_{Si}^{+}V_n^{-} \rightarrow O_{Si}^{+2}V_n^{-} + e^{-} \qquad (3)$$

This model implies that the activation of oxygen donors does not depend only on oxygen concentration but requires the presence of vacancies. However, since the oxygen concentration fluctuates significantly in Si crystals, this implication could not be tested without knowledge of the actual concentration of oxygen on a microscale.

The present results show that the concentration of activated donors may not be proportional to the oxygen concentration. In the light of the model this result is not surprising since the distribution (or availability) of vacancies does not necessarily coincide with the oxygen distribution. During heat treatment at 650°C diffusion makes more vacancies available to the oxygen sites; thus upon subsequent heat treatment at 450°C (consistent with the present experimental results) activation of donors can take place in regions where vacancies are not available and activation could not have taken place; on the other hand, in regions where activation had taken place, additional vacancies, V_f, render the activated donor electrically inert by forming inert stable complexes as follows:

$$O_{Si}^{+}V_n^{-} + V_f \rightarrow O_{Si}^{+2}V_n^{-}V_f^{-} \qquad (4)$$

Although the annihilation of thermal donors at 650°C is not entirely clear at present, it is possible that the bonding of the donor complex is altered to an electrically inert configuration. According to the authors of the above model (ref. 7) this process can be viewed as a low-energy phase transition probably due to elastic recovery processes and thus correlated to vacancy-supported stability of substitutional oxygen.

Regarding the donor activation behavior near the periphery of the crystal it is very likely that it is associated with the distribution of swirl microdefects in dislocation-free crystals. It has been reported (ref. 8) that high density of microdefects (vacancy clusters) is present near the periphery of the crystals (referred to as B-type). These defects are essentially vacancy getters and thus extensive activation of donors does not take place in this region of the crystal until prolonged heat treatment at 650°C releases vacancies from these clusters which then participate in donor activation. The density of this type of clusters becomes significantly smaller away from the crystal periphery. On the other hand, the type of microdefects present towards

the center of the crystals, referred to as A-type, are larger than the B-type and may not constitute active vacancy clusters.

It should be pointed out that not only vacancies, but also acceptor atoms, play a role in the activation of oxygen donors. Preliminary results in our laboratory with p-type crystals doped with acceptors other than B(e.g., Al, In and Ga) indicate that the donor activation rates are different for the different dopant elements. This work is currently being pursued further.

In summary, we have shown that thermal oxygen donor formation is not controlled solely by the oxygen concentration. The equally important role of vacancies in this process was clearly demonstrated by direct microscale analysis of oxygen and thermal donor concentrations.

REFERENCES

1. A.Murgai, H.C. Gatos, W.A. Westdorp, J. Electrochem. Soc. 126, 2240 (1979); A. Murgai, J.Y. Chi and H.C. Gatos, J. Electrochem. Soc. 127, 1182 (1980).

2. W. Kaiser, H.L. Frisch and H. Reiss, Phys. Rev. 112, 1546 (1958).

3. A. Ohsawa, K. Honda, S. Ohkawa and R. Ueda, Appl. Phys. Lett. 36, 147 (1980).

4. L. Jastrzebski, J. Lagowski and H.C. Gatos, J. Electrochem. Soc. 126, 260 (1979).

5. W. Walukiewicz, J. Lagowski, L. Jastrzebski, P. Rava, M. Lichtensteiger, C.H. Gatos and H.C. Gatos, J. Appl. Phys. 51, 2659 (1980).

6. Standard test method for interstitial atomic oxygen content of silicon by infrared absorption, ASTM Standard F 121-76.

7. D. Helmreich and E. Sirtl, Semiconductor Silicon, 1977, edited by H.R. Huff and E. Sirtl, Electrochem. Soc., p. 626.

8. A.J.R. De Kock, Philips Res. Repts. Suppl. 1973, No. 1.

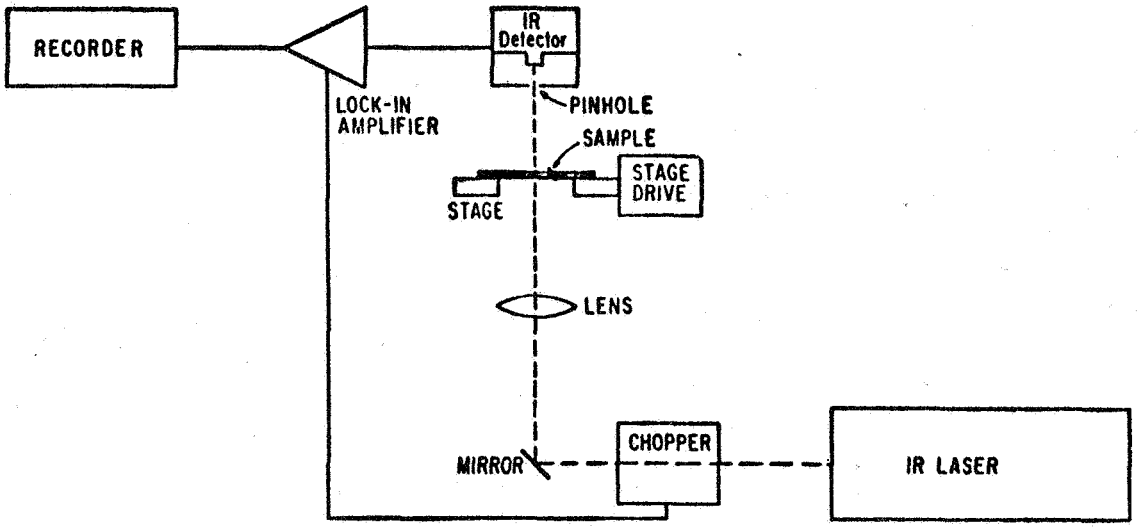

Figure 1. Schematic representation of IR scanning apparatus for oxygen microprofiling.

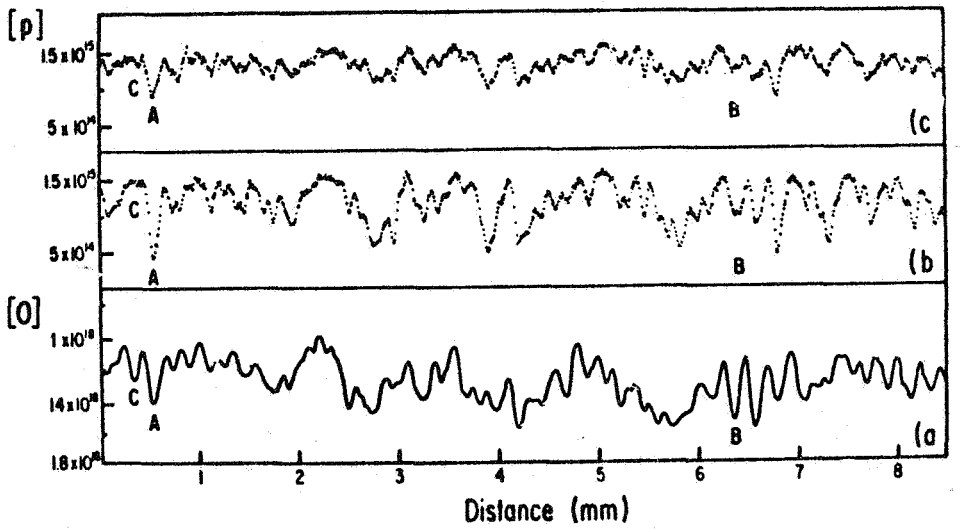

Figure 2. (a) Oxygen concentration, [O], (O/cm^3) as a function of distance parallel to the direction of growth at a distance of 6 mm from the periphery of the crystal obtained by scanning IR absorption. (b) Hole concentration, [p], (p/cm^3) obtained with spreading resistance measurements along the same location as in (a) after 4 hrs heat treatment at 450°C. (c) Hole concentration along the same location as in (a) after 4 hrs heat treatment at 450°C followed by heat treatments for 4 hrs at 650°C and 8 hrs at 450°C.

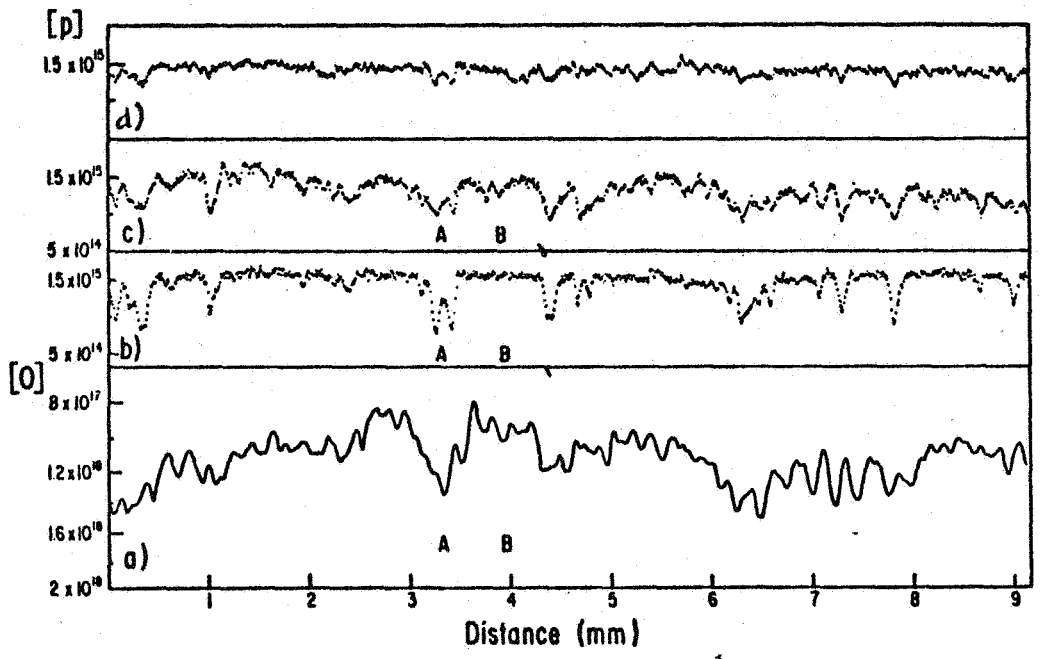

Figure 3. (a) Oxygen concentration, [O], (O/cm^3) as a function of distance parallel to the direction of growth at a distance 4.5 mm from the periphery of the crystal obtained by scanning IR absorption. (b) Hole concentration, [p], (p/cm^3) obtained with spreading resistance measurements along the same location as in (a) after 4 hrs heat treatment at 450°C. (c) Hole concentration along the same direction as in (a) after 4 hrs heat treatment at 450°C followed by heat treatment for 4 hrs at 650°C and 8 hrs at 450°C. (d) Hole concentration as in (c) after following heat treatments for 4 hrs at 650°C and 8 hrs at 450°C.

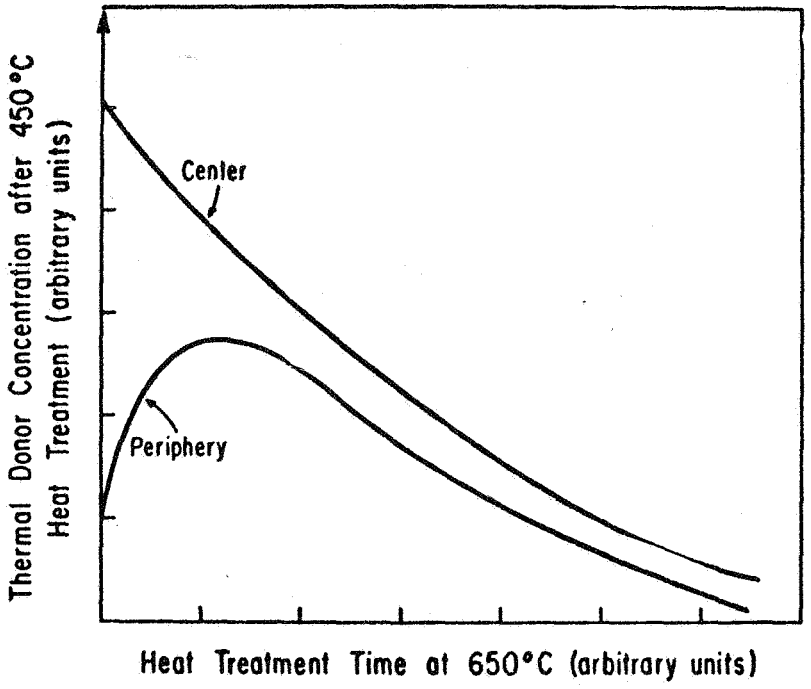

Figure 4. Thermal donor concentration after heat treatment cycles at 450°C, 650°C, 450°C as a function of cumulative 650°C heat treatment times.

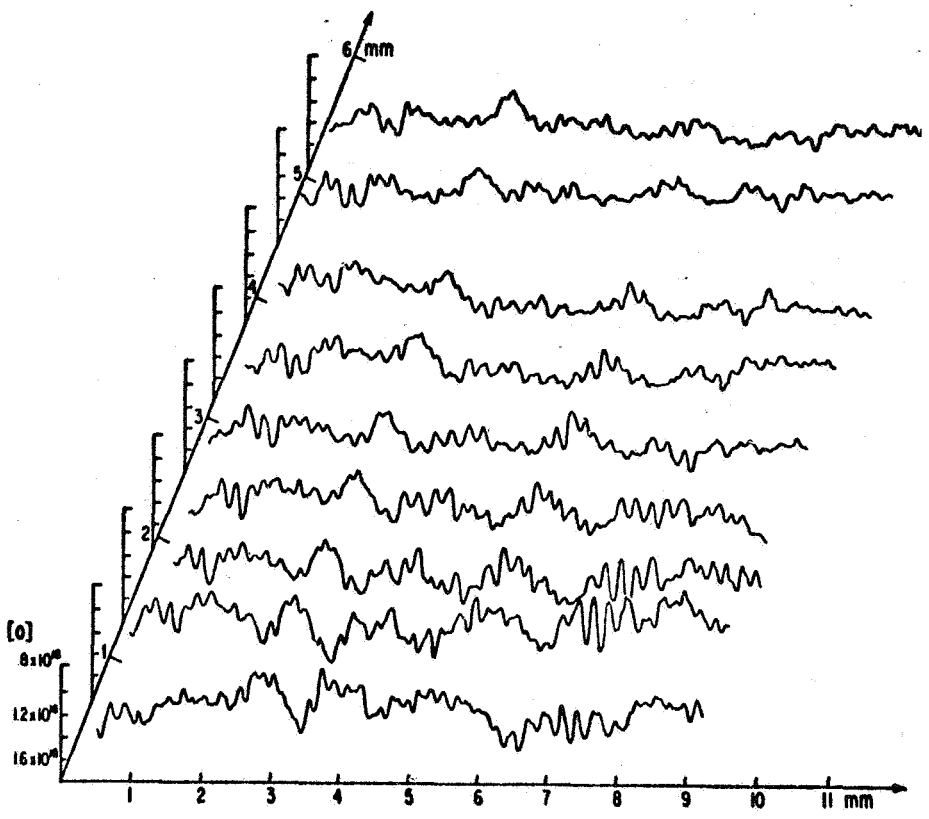

Figure 5. Oxygen profiles in a silicon crystal at various locations (abscissa) from the periphery towards the center of the crystal.

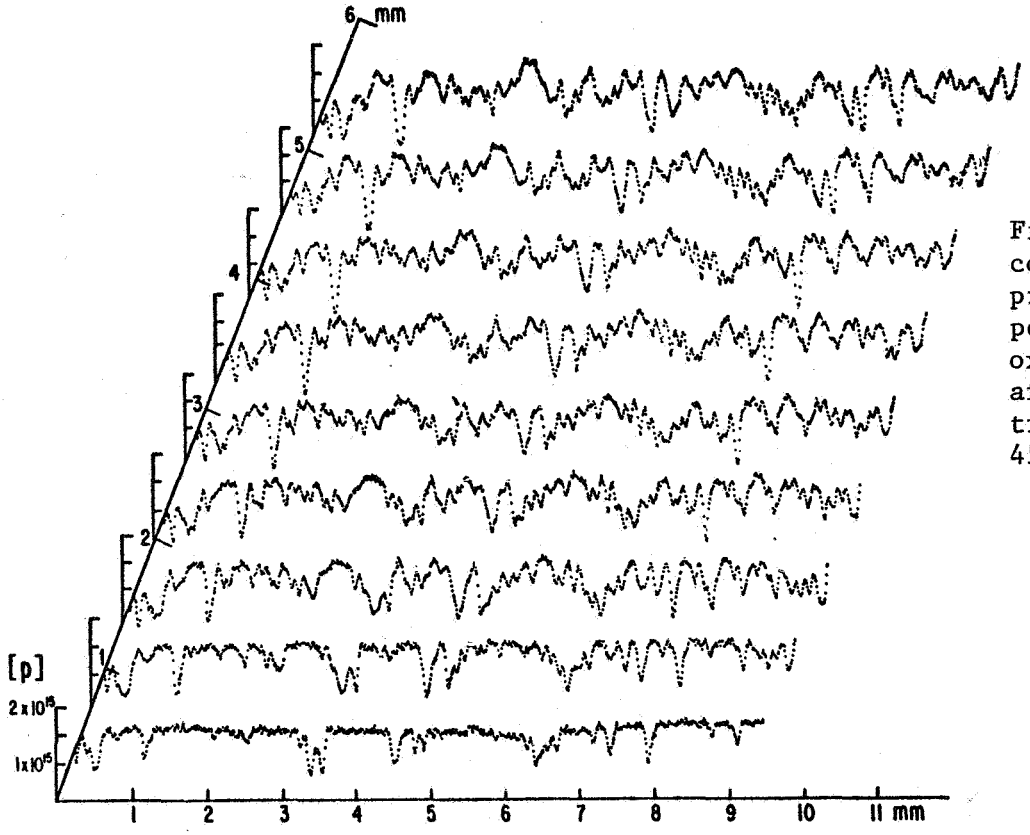

Figure 6. Carrier concentration profiles corresponding to the oxygen profiles after heat treatment at 450°C for 4 hrs.